

Article

Dynamic Analytical Solution of a Charged Dilaton Black Hole

Ruifang Wang , Jianwen Liu  and Fabao Gao * 

School of Mathematical Science, Yangzhou University, Yangzhou 225002, China; wangruifang16@sina.com (R.W.); liuwenjie@163.com (J.L.)

* Correspondence: fbgao@yzu.edu.cn or gaofabao@sina.com

Abstract: This paper addresses an analytic solution of the particles in a charged dilaton black hole based on the two-timing scale method from the perspective of dynamics. The constructed solution is surprisingly consistent with the “exact solution” in the numerical sense of the system. It can clearly reflect how the physical characteristics of the particle flow, such as the viscosity, absolute temperature, and thermodynamic pressure, affect the characteristics of the black hole. Additionally, we also discuss the geometric structure relationship between the critical temperature and the charge as well as the dilaton parameter when a charged dilaton black hole undergoes a phase transition. It is found that the critical temperature decreases with the increase of the charge for a given dilaton value. When the charge value is small, the critical temperature value will first decrease and then increase as the dilaton value increases. Conversely, the critical temperature value will always increase with the dilaton parameter.

Keywords: dynamic analytical solution; charged dilaton black hole; two-timing scale method; critical temperature

MSC: 37M20; 65P30; 85A40



Citation: Wang, R.; Liu, J.; Gao, F.

Dynamic Analytical Solution of a Charged Dilaton Black Hole.

Mathematics **2022**, *10*, 2113. <https://doi.org/10.3390/math10122113>

Academic Editors: Stoytcho Stoyanov Yazadjiev and Petya Nedkova

Received: 21 May 2022

Accepted: 15 June 2022

Published: 17 June 2022

Publisher's Note: MDPI stays neutral with regard to jurisdictional claims in published maps and institutional affiliations.



Copyright: © 2022 by the authors. Licensee MDPI, Basel, Switzerland. This article is an open access article distributed under the terms and conditions of the Creative Commons Attribution (CC BY) license (<https://creativecommons.org/licenses/by/4.0/>).

1. Introduction

The invisible black hole is an important part of the physical reality of our galaxy and the entire universe [1]. On studying the evolution of black holes satisfying the Starobinsky model under $f(R)$ gravity, Pati et al. [2] found that the model can explain the universe's accelerating expansion based on power-law cosmology. Many studies have proved that the Anti-de Sitter (AdS) black hole exhibits similar thermodynamic behavior to the van-der Waals fluid system. Furthermore, the profound relationship between the charged AdS black hole and van-der Waals fluid system is stated by proving that the mass of the former is a function of the charge [3]. This fact was supported in Ref. [4], and the extended method of studying the critical behavior of charged AdS black holes can be used in all high-dimensional cases. Moreover, the Gauss–Bonnet black hole was also studied by giving its equation of state, Gibbs free energy, and the critical behavior of the black hole system [4]. There are also many studies about the thermodynamics of various black holes as follows. The thermodynamics of the higher-dimensional Reissner–Nordström–de Sitter black hole, Jordan frame scalar-tensor black hole, rotating black branes, and the regular and the Bardeen–AdS black hole in Einstein–Gauss–Bonnet theory were studied respectively in Refs. [5–9]. For the Born–Infeld (BI) black hole in a cavity, Wang et al. [10] studied its thermodynamic behavior and phase diagrams different from typical BI black holes. They also studied the critical behavior and the phase structure of the BI–AdS black holes and the thermodynamics of nonlinear electrodynamics AdS black holes [11]. The study of the $(2 + 1)$ -dimensional regular black holes with nonlinear electrodynamics sources and topological dilatonic Lifshitz-like black holes can be found in Refs. [12,13].

In recent years, the study of black hole thermodynamics in the extended phase space also attracted many researchers [14–25]. In addition, various black holes may admit dif-

ferent solutions. The methods to obtain these solutions, including the exact techniques and approximate methods, were summarized in Ref. [26], which helps us know the black hole solutions comparatively. By considering the Einstein–Maxwell-dilaton theory and the Einstein-dilaton gravity theory coupled to the BI nonlinear electrodynamics, the static and dynamic charged black holes were set up [27,28]. For the rotating regular black hole and the charged AdS black hole in different dimensions, their solutions were proposed by considering the Newman–Janis algorithm and the massive gravity theory [29–31]. Based on the $(2 + 1)$ -dimensional Reissner–Nordström black hole, three black hole solutions were derived by considering diverse nonlinear electromagnetic fields [32]. While in $(1 + 1)$ -dimensional non-projectable Hořava–Lifshitz gravity, the ordinary black hole has related solutions [33]. The solutions to the dilatonic dyon black hole, the anyon black hole, charged rotating dilaton, other various dilaton black holes, and the black holes with nonlinear electrodynamic field and a Kalb–Ramond field can be found in Refs. [34–44]. A new study gave the exact solutions of static spherical symmetry in the interaction of aether and Einstein-aether scalar field, which describe hairy black hole solutions [45]. These solutions are helpful for researchers to understand the properties of black holes further.

Whether the parameters involved in different black holes affect the system is also a significant problem. In the extended phase space, the influence of the perturbation of the cosmological constant, the charge, and the massive gravity was analyzed for the black holes with the background of charged Hořava–Lifshitz and massive gravity [46,47]. For the black hole in de Rham, Gabadadze, and Tolley’s massive gravity in new extended phase space, the influence of distinct values of the spacetime parameters on the thermodynamic stability was also presented [48]. In the Schwarzschild black hole, the cosmological constant has a significant influence on the dynamics of the neutral and charged particles, and it is also a necessary condition for accelerating the expansion of the universe [49]. Furthermore, the spin parameter and dimensionless parameter in the modified theory of gravity can affect the motion of particles near a rotating black hole [50]. In addition, some other researchers have also discussed the freedom in specifying the physical parameters of multiple black hole configurations [51] and the influence of external sources on the behavior of the perturbed black holes [52–54].

At present, there are many references on the periodic orbits around various black holes, which are helpful to the study of the particle’s motion of the charged dilaton black hole [55,56]. In the background of the four-dimensional Einstein–Gauss–Bonnet black holes, Zhang et al. [57] analyzed the motion of a spinning test particle and found that a discrete gravitational radiation spectrum will appear when the particle is inhaled in these black holes. By focusing on the periodic motion of a timelike particle around the Dadhich, Maartens, Papadopoulos, and Rezanian brane-world black holes, Deng [58] found that for different values of the tidal charge parameter, the periodic orbits have different energy. For the Schwarzschild black hole and the high-dimensional black hole, the dynamical behavior of the particles was studied, including the escape velocity and retrograde trajectory of particles [55,59,60]. For Kehagias–Sfetsos black holes in deformed Hořava–Lifshitz gravity, their periodic orbits were studied based on the marginally bound and innermost stable circular orbits. The energy of these periodic orbits, which is lower than that of a Schwarzschild black hole, is related to the parameter in Hořava–Lifshitz gravity [61–63]. The zoom-whirl periodic orbits around the Kerr–Sen black hole were considered, and the effect of the charge parameter on these orbits was also discussed. The energy of these periodic orbits is found lower than those of the Kerr black hole [64]. In addition, some physicists pay attention to the quasi-periodic oscillations in the stellar-mass black hole binaries [65,66].

Inspired by the above studies on black hole solutions and black hole thermodynamics in extended phase space, this paper will study the physical phase transitions in the spacetime background of charged dilaton black holes and the dynamic behavior of black holes in extended phase space from the perspective of nonlinear dynamics. The dynamic analytical solution of the charged dilaton black hole is studied by adopting the two-timing scale

method (see [67] for more details). This method is an effective method for quantitative analysis of nonlinear dynamics. It can not only describe periodic motion but also show the attenuated vibration of the dissipative system. In addition, we will also study the thermodynamic properties of the charged dilaton black hole and the time-dependent behavior of this black hole system in an unstable state. The layout of the paper is as follows. Section 2 will introduce the nonlinear dynamical equation of the charged dilaton black hole in the extended phase space. In Section 3, the two-timing scale method will be used to solve the system, and the numerical comparison will be carried out in Section 4. Finally, the paper draws a conclusion.

2. Dynamical Equation in Extended Phase Space

2.1. Thermodynamic Equation

In the extended phase space, we will briefly review the thermodynamics of a charged dilaton black hole. The action of Einstein–Maxwell theory with a dilation field in four-dimensional spacetime is as follows

$$I = \frac{1}{16\pi} \int d^4x \sqrt{-g} \left[R - 2(\nabla\phi)^2 - 2\Lambda e^{2\alpha\phi} - \frac{2\alpha^2}{b^2(\alpha^2 - 1)} e^{2\phi/\alpha} - e^{-2\alpha\phi} F_{\mu\nu} F^{\mu\nu} \right], \quad (1)$$

where ϕ is the scalar field of dilaton, Λ is the cosmological constant, $F_{\mu\nu} = \partial[\mu A_{\nu]}$ is the electromagnetic tensor related to vector potential A_ν , μ is a small positive constant viscosity, α is the coupling parameter between the Maxwell and dilaton fields, and b is an arbitrary positive constant (see [68–72] for more details).

According to the action Equation (1), one can obtain the following metric element describing the spherical symmetric black hole solution

$$ds^2 = -f(r)dt^2 + \frac{1}{f(r)}dr^2 + r^2R(r)^2(d\theta^2 + \sin^2\theta d\phi^2), \quad (2)$$

with

$$f(r) = -\frac{\alpha^2 + 1}{\alpha^2 - 1} \left(\frac{b}{r}\right)^{-2\gamma} - \frac{m}{r^{1-2\gamma}} - \frac{3(\alpha^2 + 1)^2 r^2}{l^2(\alpha^2 - 3)} \left(\frac{b}{r}\right)^{2\gamma} + \frac{q^2(\alpha^2 + 1)}{r^2} \left(\frac{b}{r}\right)^{-2\gamma},$$

$$\phi(r) = \frac{\alpha}{\alpha^2 + 1} \ln\left(\frac{b}{r}\right), \quad R(r) = \left(\frac{b}{r}\right)^\gamma,$$

where $\gamma = \alpha^2/(\alpha^2 + 1)$, q is the black hole charge, and $m = 2(\alpha^2 + 1)b^{-2\gamma}M$ is related to the ADM mass M of Equation (2) (see [68,69]). This metric depicts the geometry of the Reissner–Nordström black hole when there is no dilaton field (i.e., $\alpha = 0$).

Considering the thermodynamic pressure P and the volume V , which are conjugated quantities, have the following form

$$P = -\frac{(3 + \alpha^2)b^{2\gamma}\Lambda}{8\pi(3 - \alpha^2)r_+^{2\gamma}}, \quad (3)$$

$$V = \frac{4\pi(1 + \alpha^2)b^{2\gamma}}{3 + \alpha^2} r_+^{\frac{3+\alpha^2}{1+\alpha^2}}, \quad (4)$$

where r_+ is the largest root of the equation $f(r) = 0$, which is the event horizon radius. Note that the cosmological constant Λ is integrated into the pressure P (refer to [73,74] for more details). According to the Smarr formula and the first law of thermodynamics, then P and V in Equations (3) and (4) can be simplified as

$$P = -\frac{\Lambda}{8\pi}, \quad V = \frac{4\pi r_+^3}{3}.$$

which are in agreement with the Reissner–Nordström black hole. For a given specific volume

$$v = \frac{2(1 + \alpha^2)(3 - \alpha^2)}{(3 + \alpha^2)}r_+,$$

then the pressure P becomes

$$P(v, T) = \frac{T}{v} + \frac{b^{-2\gamma}}{2^{2\gamma}\pi v^{2(1-\gamma)}(\alpha^2 + 1)^{2(\gamma-2)}} \times \left[\frac{(3 - \alpha^2)^{1-2\gamma}}{2(\alpha^2 - 1)(\alpha^2 + 1)^2(3 + \alpha^2)^{1-2\gamma}} + \frac{2q^2(3 + \alpha^2)^{2\gamma-3}}{v^2(3 - \alpha^2)^{2\gamma-3}} \right].$$

Moreover, the second-order phase transition of the black hole (2) occurs at the critical temperature

$$T_c = \frac{(\alpha^2 + 1)(3 + \alpha^2)^{\frac{2\gamma-3}{2}}}{\pi b^{2\gamma} q^{1-2\gamma} (1 - \alpha^2)(\alpha^2 + 2)^{\frac{1-2\gamma}{2}}}.$$

The relationships among the parameter b , the charge q , the dilaton parameter α and the critical temperature T_c are shown in Figures 1–4. For a given value of α , the critical temperature T_c decreases with the increasing of the charge q for each parameter b . Similarly, the value of T_c also decreases with the increasing of parameter b for each value of q (see Figure 1). Additionally, when q value is small, the T_c - α curve declines visibly, after that it rises with the increasing of α , which presents parabolic type (see Figure 2). Additionally, we find that with the increasing of q , the T_c and α corresponding to the lowest point of T_c - α curve are decreasing. While when the value of q becomes large, for instance $q = 1$, the value of T_c increases with the increasing of α (see Figures 2 and 3). Then take the critical temperature $T_c = 0.3$, the relationship between q , α and b is given in Figure 4, which illustrates that there is a complex relationship between these three parameters.

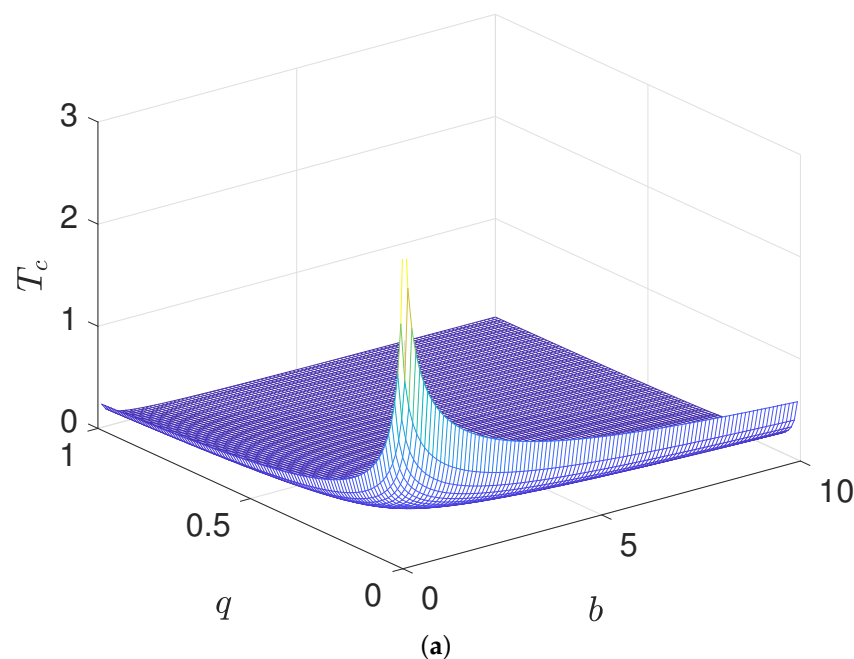


Figure 1. Cont.

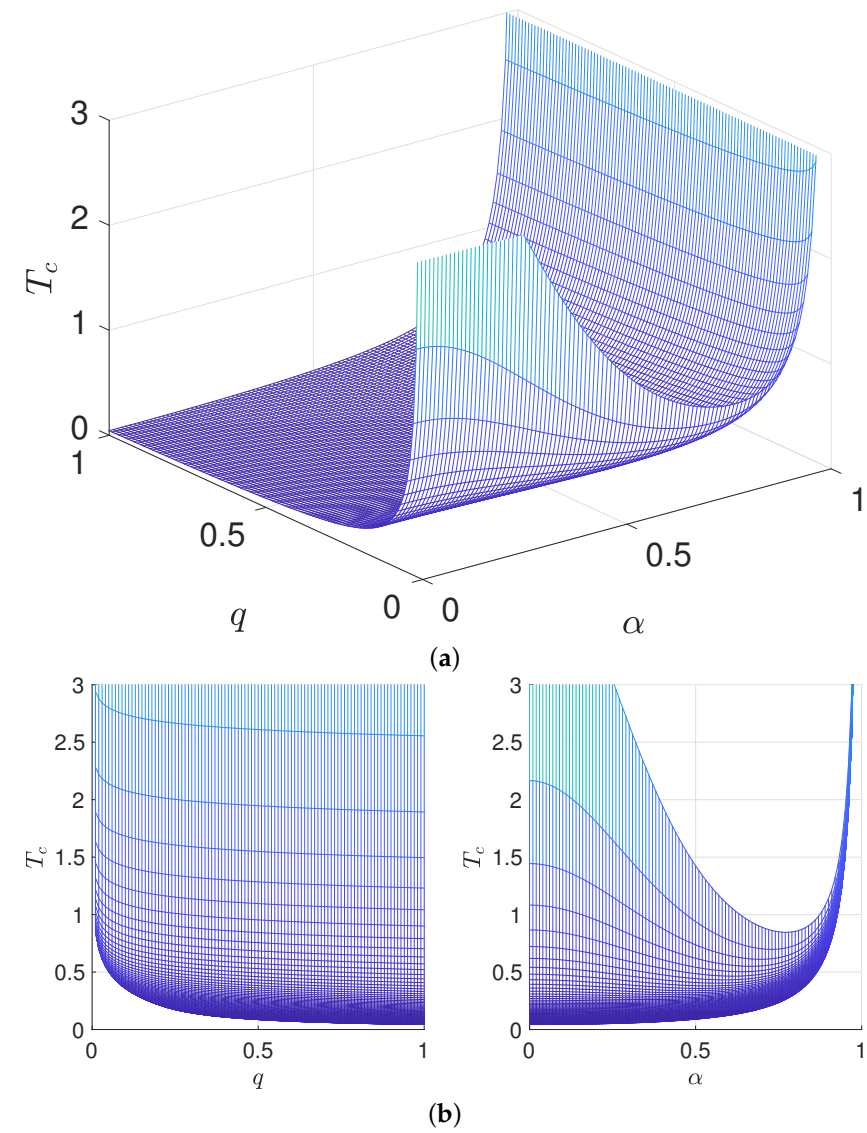
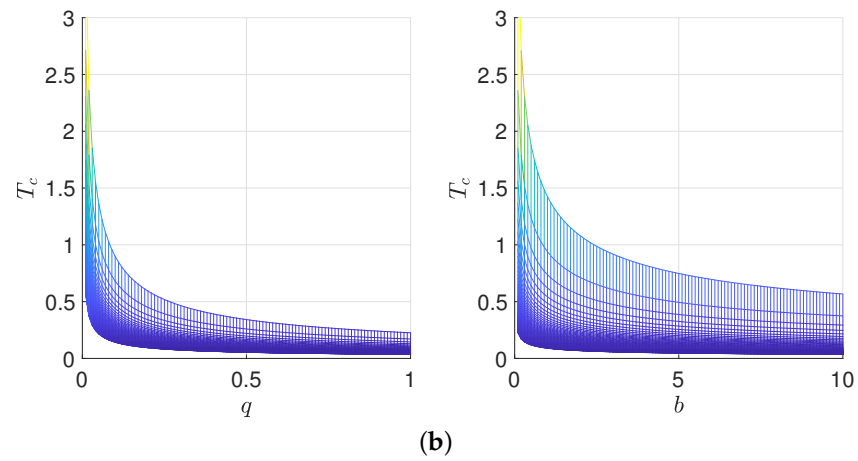


Figure 2. The relationship between the critical temperature T_c , the charge q and the dilaton parameter α : (a) T_c - q - α relationship diagram, (b) T_c - q and T_c - α relationship diagrams.

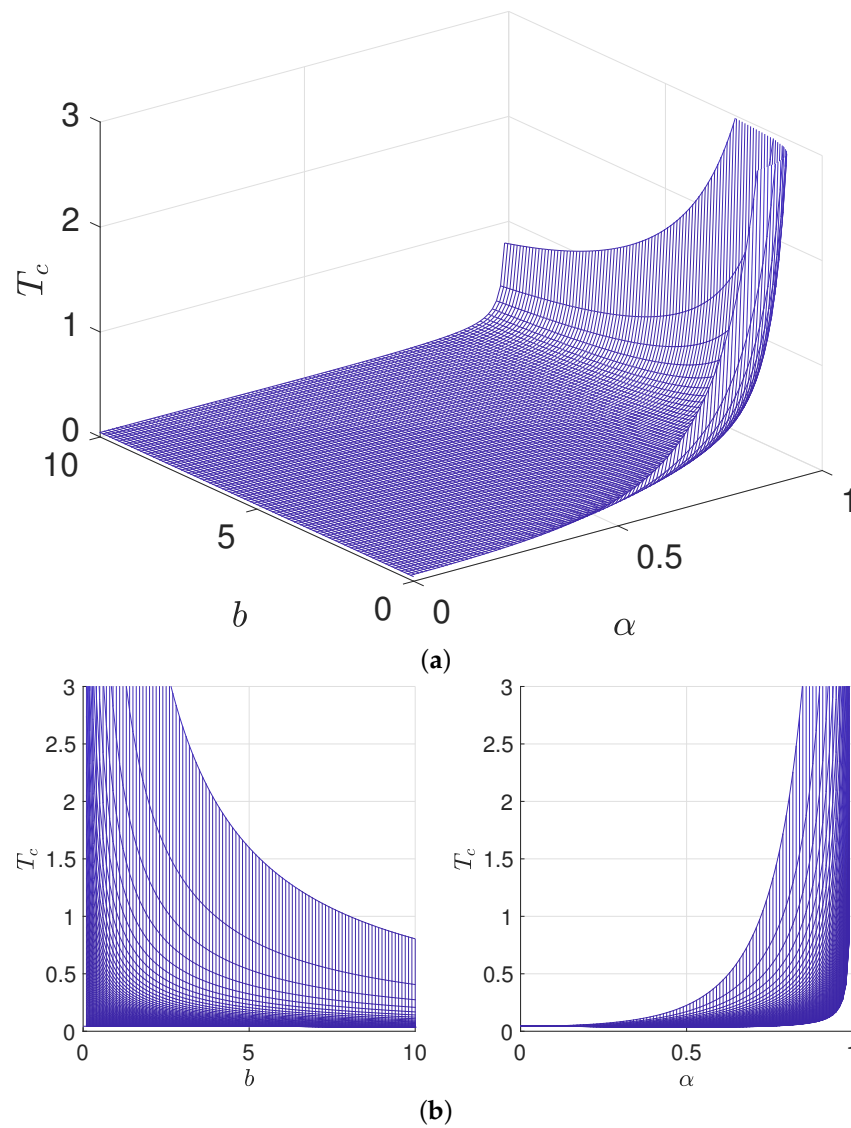


Figure 3. The relationship between the critical temperature T_c , the dilaton parameter α and the parameter b : (a) T_c - b - α relationship diagram, (b) T_c - b and T_c - α relationship diagrams.

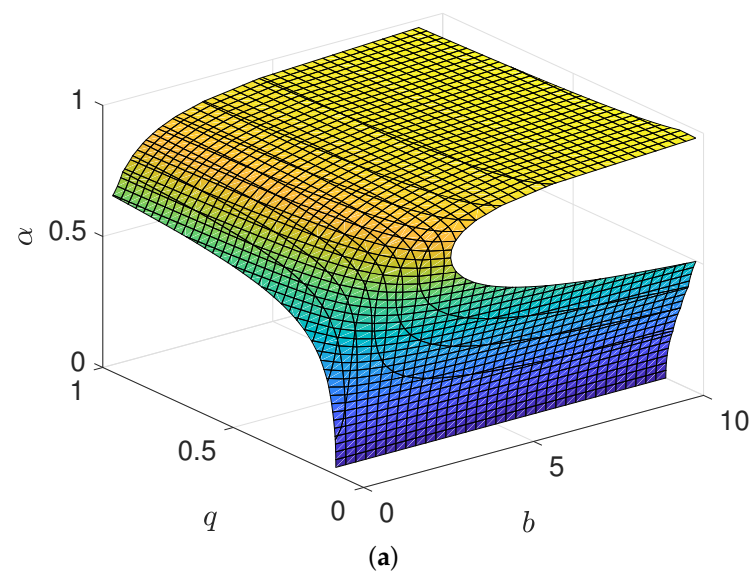


Figure 4. Cont.

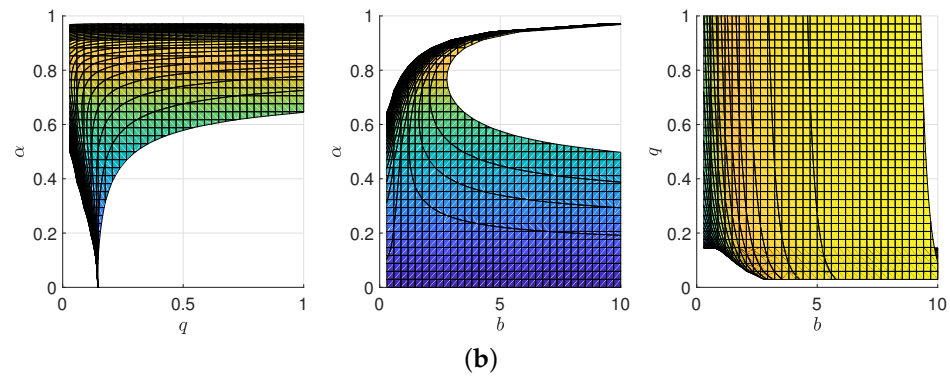


Figure 4. The relationship between the charge q , the dilaton parameter α and the parameter b when the critical temperature $T_c = 0.3$: (a) α - q - b relationship diagram, (b) α - q , α - b and q - b relationship diagrams.

2.2. Dynamical Balance Equation

It is assumed that the charged dilaton black hole flow moves in a tube with a fixed volume and unit cross-section. The position of particles can be characterized by Eulerian coordinate $x = x(M, t)$, where M is the mass of the column of fluid of unit cross-section between a fluid particle and the reference fluid particle, and t is time. Then the specific volume and the velocity of the particle can be obtained by $v(M, t) = \partial x(M, t) / \partial M$ and $u(M, t) = \partial x(M, t) / \partial t$, respectively. Assuming that the fluid here is thermoelastic, slightly viscous, and isotropic, then it can be described by the following equation

$$x_{tt} = -P(v, T)_M + \epsilon \mu_0 s u_{MM} - A s^2 v_{MMM}, \tag{5}$$

where $x_{tt} = \partial^2 x / \partial t^2$, $P(v, T)_M = \partial P(v, T) / \partial M$, $u_{MM} = \partial^2 u / \partial M^2$, $v_{MMM} = \partial^3 v / \partial M^3$, $\epsilon (0 < \epsilon \ll 1)$ is a thermal perturbation parameter, μ_0 is a positive parameter related to the viscosity, s is a positive parameter, and A is a positive constant (see Ref. [68] for more detail).

Assume that the total mass of the black hole fluid tube with a volume of $2\pi v_0 / s$ and a unit cross-section is $2\pi / s$, where v_0 is the inflection point determined by $\partial^2 P / \partial v^2 = 0$. Consider that the absolute temperature T has a slight periodic fluctuation (see [75–77] for details) in the form of

$$T = T_0 + \epsilon \delta \cos(\omega t) \cos M,$$

where δ is the perturbation amplitude relative to the small viscosity, ω is frequency of T , and $T_0 < T_c$.

Note that the functions $v(M, t)$ and $u(M, t)$ can be respectively expanded into Fourier series

$$\begin{aligned} v(M, t) &= v_0 + x_1(t) \cos M + x_2(t) \cos 2M + x_3(t) \cos 3M + \dots, \\ u(x, t) &= u_1(t) \sin M + u_2(t) \sin 2M + u_3(t) \sin 3M + \dots, \end{aligned}$$

with respect to $M \in [0, 2\pi]$ near the inflection point v_0 , where $x_i(t)$ and $u_i(t)$, which are regarded as hydrodynamical modes, can be described as the deviation of the initial equilibrium state. Consider the first mode $(x_1(t), u_1(t))$. For convenience, we omit the subscript 1 below. In this way, the dynamical Equation (5) can be reduced to (omit (v_0, T_0))

$$\begin{aligned} \dot{x} &= u, \\ \dot{u} &= \left(P_v - A s^2 \right) x + \epsilon \left(P_T + \frac{3 P_{vvT}}{8} x^2 \right) \delta \cos \omega t + \frac{P_{vvv}}{8} x^3 - \epsilon \mu_0 s u, \end{aligned}$$

where

$$\begin{aligned}
 P(v, T) = & P(v_0, T_0) + P_v(v_0, T_0)(v - v_0) + P_T(v_0, T_0)(T - T_0) \\
 & + P_{vT}(v_0, T_0)(v - v_0)(T - T_0) + \frac{P_{vvv}(v_0, T_0)}{3!}(v - v_0)^3 \\
 & + \frac{P_{vvT}(v_0, T_0)}{2}(v - v_0)^2(T - T_0) + \dots,
 \end{aligned}$$

with

$$\begin{aligned}
 P_T(v_0, T_0) &= \frac{1}{v_0}, \quad P_{vT}(v_0, T_0) = -\frac{1}{v_0^2}, \quad P_{vvT}(v_0, T_0) = \frac{2}{v_0^3}, \\
 P_v(v_0, T_0) &= -\frac{T_0}{v_0^2} + \frac{[(3 - \alpha^2)(\alpha^2 + 1)]^{\frac{1-\alpha^2}{\alpha^2+1}}}{\pi(1 - \alpha^2)4^{\frac{\alpha^2}{\alpha^2+1}}b^{\frac{2\alpha^2}{\alpha^2+1}}(\alpha^2 + 3)^{\frac{\alpha^2+3}{\alpha^2+1}}v_0^{\frac{3\alpha^2+5}{\alpha^2+1}}} \\
 &\quad \times \left[4(\alpha^4 + \alpha^2 - 2)(\alpha^4 - 2\alpha^2 - 3)^2 q^2 + (\alpha^2 + 3)^2 v_0^2 \right], \\
 P_{vvv}(v_0, T_0) &= -\frac{6T_0}{v_0^4} + \frac{2(3 - \alpha^2)^{\frac{1-\alpha^2}{1+\alpha^2}}(\alpha^2 + 2)}{\pi(1 - \alpha^2)4^{\frac{\alpha^2}{\alpha^2+1}}b^{\frac{2\alpha^2}{\alpha^2+1}}(\alpha^2 + 1)^{\frac{3\alpha^2+1}{\alpha^2+1}}(\alpha^2 + 3)^{\frac{\alpha^2+3}{\alpha^2+1}}v_0^{\frac{5\alpha^2+7}{\alpha^2+1}}} \\
 &\quad \times \left[(\alpha^2 + 3)^3 v_0^2 + 4(\alpha^2 - 1)(2\alpha^2 + 3)(3\alpha^2 + 5)(\alpha^4 - 2\alpha^2 - 3)^2 q^2 \right].
 \end{aligned}$$

Note that we have found that the expression for $P_{vvv}(v_0, T_0)$ here is different from that derived in Ref. [68] after repeated verification.

Now the dynamical equation of the charged dilaton black hole flow can be written as

$$\frac{d^2x}{dt^2} + \epsilon\mu_0s \frac{dx}{dt} + (As^2 - P_v)x - \epsilon \left(P_T + \frac{3P_{vvT}}{8}x^2 \right) \delta \cos \omega t - \frac{P_{vvv}}{8}x^3 = 0. \tag{6}$$

3. Analytical Solution of Dynamics

In this section, we will construct a uniformly valid expansion of the perturbation problem of Equation (6) by using the well-known two-timing method in the field of nonlinear dynamics, to study the periodic thermal behavior of the black hole in the extended phase space. To this end, we suppose that the asymptotic solution of Equation (6) is expressed in terms of the thermal perturbation parameter ϵ as defined by

$$x(t, \epsilon) = \epsilon x_1(T_1, T_2) + \epsilon^2 x_2(T_1, T_2), \tag{7}$$

where $T_1 = t, T_2 = \epsilon t$ are fast and slow time scales, respectively.

By the chain rule, define

$$\begin{aligned}
 \frac{dx_i}{dt} &= \frac{dx_i}{dT_1} \cdot \frac{dT_1}{dt} + \frac{dx_i}{dT_2} \cdot \frac{dT_2}{dt} \\
 &= \frac{dx_i}{dT_1} + \epsilon \cdot \frac{dx_i}{dT_2} \\
 &\triangleq \partial_{T_1} x_i + \epsilon \partial_{T_2} x_i,
 \end{aligned} \tag{8}$$

$$\begin{aligned}
 \frac{d^2x_i}{dt^2} &= \frac{d}{dt} \left(\frac{dx_i}{dT_1} + \epsilon \cdot \frac{dx_i}{dT_2} \right) \\
 &= \frac{d^2x_i}{dT_1^2} + 2\epsilon \cdot \frac{d^2x_i}{dT_1 dT_2} + \epsilon^2 \cdot \frac{d^2x_i}{dT_2^2} \\
 &\triangleq \partial_{T_1 T_1} x_i + 2\epsilon \partial_{T_1 T_2} x_i + \epsilon^2 \partial_{T_2 T_2} x_i,
 \end{aligned} \tag{9}$$

where $i = 1, 2$. Then substituting Equations (7)–(9) into Equation (6) and comparing the coefficients of powers of ϵ , we have

$$\epsilon^1 : \partial_{T_1 T_1} x_1 + (As^2 - P_v)x_1 = P_T \delta \cos(\omega T_1), \tag{10}$$

$$\epsilon^2 : \partial_{T_1 T_1} x_2 + (As^2 - P_v)x_2 = -2\partial_{T_1 T_2} x_1 - \mu_0 s \partial_{T_1} x_1, \tag{11}$$

$$\begin{aligned} \epsilon^3 : \partial_{T_1 T_1} x_3 + (As^2 - P_v)x_3 = & -\partial_{T_2 T_2} x_1 - 2\partial_{T_1 T_2} x_2 - \mu_0 s (\partial_{T_2} x_1 + \partial_{T_1} x_2) \\ & + \frac{3P_{vvT} \delta \cos(\omega T_1)}{8} x_1^2 + \frac{P_{vvv}}{8} x_1^3. \end{aligned} \tag{12}$$

Note that the homoclinic orbits of Equation (6) has been discussed in Ref. [68] for the case $(As^2 - P_v) \leq 0$. We now consider the case $(As^2 - P_v) > 0$ and assume that $\omega^2 \neq (As^2 - P_v)$ to avoid the resonance, and write the solution of Equation (10) in the following form

$$\begin{aligned} x_1(T_1, T_2) = & K(T_2)e^{i\sqrt{As^2 - P_v}T_1} + \overline{K(T_2)}e^{-i\sqrt{As^2 - P_v}T_1} \\ & - \frac{P_T \delta}{2(\omega^2 - As^2 + P_v)} (e^{i\omega T_1} + e^{-i\omega T_1}), \end{aligned} \tag{13}$$

where \overline{K} donates the conjugate quantity of K . Substituting Equation (13) into Equation (11), we obtain

$$\begin{aligned} \partial_{T_1 T_1} x_2 + \lambda^2 x_2 = & -2i\lambda e^{i\lambda T_1} \partial_{T_2} K + 2i\lambda e^{-i\lambda T_1} \partial_{T_2} \overline{K} - \mu_0 s \left[Ki\lambda e^{i\lambda T_1} \right. \\ & \left. - \overline{K}i\lambda e^{-i\lambda T_1} - \frac{P_T \delta i\omega}{2(\omega^2 - \lambda^2)} (e^{i\omega T_1} - e^{-i\omega T_1}) \right], \end{aligned} \tag{14}$$

where $\lambda = \sqrt{As^2 - P_v} > 0$.

To eliminate the secular terms of the above equation, we let

$$\begin{aligned} -2i\lambda \partial_{T_2} K - \mu_0 s i\lambda K &= 0, \\ 2i\lambda \partial_{T_2} \overline{K} + \mu_0 s i\lambda \overline{K} &= 0. \end{aligned}$$

Then we can take

$$K(T_2) = \overline{K(T_2)} = e^{-\frac{\mu_0 s}{2} T_2}.$$

Thus a special solution of Equation (10) becomes

$$x_1(T_1, T_2) = 2e^{-\frac{\mu_0 s}{2} T_2} \cos \lambda T_1 - \frac{P_T \delta}{\omega^2 - \lambda^2} \cos \omega T_1, \tag{15}$$

and Equation (14) is reduced to

$$\partial_{T_1 T_1} x_2 + \lambda^2 x_2 = -\frac{\mu_0 s P_T \delta i\omega}{2(\omega^2 - \lambda^2)} (e^{i\omega T_1} - e^{-i\omega T_1}). \tag{16}$$

Similarly, suppose that the solution of Equation (16) is

$$x_2(T_1, T_2) = L(T_2)e^{i\lambda T_1} + \overline{L(T_2)}e^{-i\lambda T_1} - \frac{\mu_0 s P_T \delta i\omega}{2(\omega^2 - \lambda^2)^2} (e^{i\omega T_1} - e^{-i\omega T_1}). \tag{17}$$

Substituting Equations (15) and (17) into Equation (12), it follows

$$\begin{aligned} \partial_{T_1 T_1} x_3 + \lambda^2 x_3 = & -\frac{\mu_0^2 s^2}{4} \left(e^{i\lambda T_1} + e^{-i\lambda T_1} \right) - 2i\lambda e^{i\lambda T_1} \partial_{T_2} L + 2i\lambda e^{-i\lambda T_1} \partial_{T_2} \bar{L} \\ & - \mu_0 s \left[-\frac{\mu_0 s}{2} e^{-\frac{\mu_0 s}{2} T_2} \left(e^{i\lambda T_1} + e^{-i\lambda T_1} \right) + i\lambda e^{i\lambda T_1} L \right. \\ & \left. - i\lambda e^{-i\lambda T_1} \bar{L} + \frac{\mu_0 s P_T \delta \omega^2}{2(\omega^2 - \lambda^2)^2} \left(e^{i\omega T_1} + e^{-i\omega T_1} \right) \right] \\ & + \frac{3P_{vv} T \delta}{16} \left(e^{i\omega T_1} + e^{-i\omega T_1} \right) x_1^2 + \frac{P_{vvv}}{8} x_1^3, \end{aligned} \tag{18}$$

where the complex expressions of x_1^2 and x_1^3 are attached in the Appendix A. Similarly, we take

$$L(T_2) = \overline{L(T_2)} = e^{-\frac{\mu_0 s}{2} T_2}.$$

Thus a particular solution of Equation (17) becomes

$$x_2(T_1, T_2) = 2e^{-\frac{\mu_0 s}{2} T_2} \cos \lambda T_1 + \frac{\mu_0 s P_T \delta \omega}{(\omega^2 - \lambda^2)^2} \sin \omega T_1.$$

Therefore, the second-order approximate solution of Equation (6) is obtained as follows

$$\begin{aligned} x = \epsilon & \left[2e^{-\frac{\mu_0 s}{2} T_2} \cos \lambda T_1 - \frac{P_T \delta}{\omega^2 - \lambda^2} \cos \omega T_1 \right] \\ & + \epsilon^2 \left[2e^{-\frac{\mu_0 s}{2} T_2} \cos \lambda T_1 + \frac{\mu_0 s P_T \delta \omega}{(\omega^2 - \lambda^2)^2} \sin \omega T_1 \right]. \end{aligned}$$

4. Numerical Comparison

In order to verify the effectiveness of the two-timing scale method, we take the same parameter values as in Ref. [68], i.e., the temperature $T_0 = 0.0315$, the charge $q = 1$, the dilaton parameter $\alpha = 0.01$ and the constant $b = 1$, then the volume $v_0 = 3.652$. For the initial condition $[-0.03226, 0]$, the numerical solution (which can be regarded as an “exact solution”) of Equation (6) and its analytical solution are shown in Figure 5. It can be seen that the solution obtained by using the two-timing scale method is much more effective for analyzing the dynamic response of the charged dilaton black hole flow. Because the changes in the blue curve and red curve are very similar, the difference between the two curves is tiny, and the two curves basically coincide. This result indicates that the asymptotic solution obtained by using this method is in good agreement with the “exact solution” of Equation (6), and these two solutions will still maintain good consistency over time.

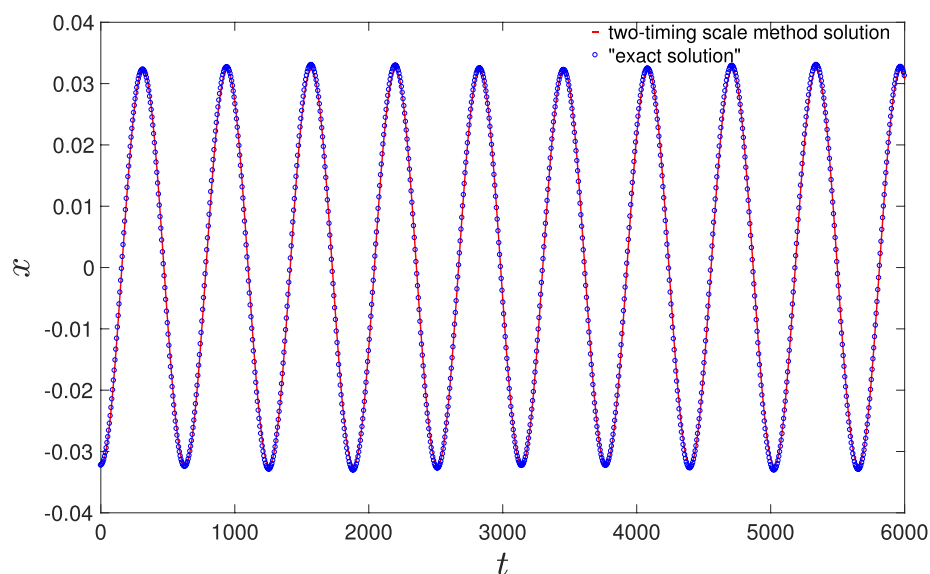


Figure 5. Comparison between the two-timing scale method solution and the “exact solution” for $A = 0.2$, $s = 0.04$, $\mu_0 = 0.1$, $\omega = 0.01$, $\delta = 0.004$, and $\epsilon = 0.001$.

5. Conclusions

The periodic thermal behavior of the charged dilaton black hole in the extended phase space was studied. For the phase transition in the black hole, i.e., the P - V critical behavior, this paper investigated the relationship between the critical temperature, the charge, and the dilaton parameter:

1. For a given value of the dilaton parameter, the critical temperature decreases with the increase of the charge;
2. For the given value of parameter b , the critical temperature value first decreases and then increases with the increase of the value of the dilaton parameter when the charge is small. On the contrary, the critical temperature value increases with the increase of the dilaton parameter value;
3. For a given value of the critical temperature, there is a complicated relationship between the charge and the dilaton parameter.

Additionally, the main innovation of this paper is that we constructed an approximate analytical solution of the nonlinear dynamic equation corresponding to the charged dilaton black hole flow from the dynamic perspective by using the two-timing scale method. The obtained solution shows surprising consistency with the numerical solution of the original system. In other words, this indicates that the obtained solution describes the dynamic behavior of the particles in the black hole flow very effectively, and the physical parameters such as viscosity, absolute temperature, and thermodynamic pressure contained in the solution can clearly reflect the dynamics of the particle in the flow. We believe this will significantly help researchers better to understand the dynamics of the charged dilaton black hole.

Author Contributions: Conceptualization, F.G.; formal analysis, R.W. and J.L.; software, R.W.; writing—original draft, R.W.; writing—review and editing, F.G. All authors have read and agreed to the published version of the manuscript.

Funding: This research was funded by the National Natural Science Foundation of China (NSFC) through grant Nos. 12172322 and 11672259, the Postgraduate Research & Practice Innovation Program of Jiangsu Province (KYCX21_3190).

Institutional Review Board Statement: Not applicable.

Informed Consent Statement: Not applicable.

Data Availability Statement: Not applicable.

Acknowledgments: We are very grateful to the anonymous reviewers whose comments and suggestions helped improve and clarify this paper.

Conflicts of Interest: The authors declare no conflict of interest.

Appendix A

The complex expressions of x_1^2 and x_1^3 in Equation (18)

$$x_1^2 = e^{-\frac{\mu_0 s}{2} T_2} e^{2i\lambda T_1} + 2e^{-\frac{\mu_0 s T_2}{2}} - \frac{e^{-\frac{\mu_0 s}{4} T_2} e^{i\lambda T_1} P_T \delta e^{i\omega T_1}}{\omega^2 - \lambda^2} - \frac{e^{-\frac{\mu_0 s}{4} T_2} e^{i\lambda T_1} P_T \delta e^{-i\omega T_1}}{\omega^2 - \lambda^2} + \frac{e^{-\frac{\mu_0 s}{2} T_2}}{e^{2i\lambda T_1}} - \frac{e^{-\frac{\mu_0 s}{4} T_2} P_T \delta e^{i\omega T_1}}{e^{i\lambda T_1} (\omega^2 - \lambda^2)} - \frac{e^{-\frac{\mu_0 s}{4} T_2} P_T \delta}{e^{i\lambda T_1} (\omega^2 - \lambda^2) e^{i\omega T_1}} + \frac{P_T^2 \delta^2 e^{2i\omega T_1}}{4(\omega^2 - \lambda^2)^2} + \frac{P_T^2 \delta^2}{2(\omega^2 - \lambda^2)^2} + \frac{P_T^2 \delta^2}{4(\omega^2 - \lambda^2)^2 e^{2i\omega T_1}}$$

$$x_1^3 = -\frac{3e^{-\frac{\mu_0 s}{2} T_2} e^{2i\lambda T_1} P_T \delta e^{i\omega T_1}}{2(\omega^2 - \lambda^2)} - \frac{3e^{-\frac{\mu_0 s}{2} T_2} e^{2i\lambda T_1} P_T \delta}{2(\omega^2 - \lambda^2) e^{i\omega T_1}} - \frac{3e^{-\frac{\mu_0 s}{2} T_2} P_T \delta e^{i\omega T_1}}{\omega^2 - \lambda^2} - \frac{3e^{-\frac{\mu_0 s}{2} T_2} P_T \delta}{(\omega^2 - \lambda^2) e^{i\omega T_1}} + \frac{3e^{-\frac{\mu_0 s}{2} T_2} e^{i\lambda T_1} P_T^2 \delta^2 e^{2i\omega T_1}}{4(\omega^2 - \lambda^2)^2} + \frac{3e^{-\frac{\mu_0 s}{4} T_2} e^{i\lambda T_1} P_T^2 \delta^2}{4(\omega^2 - \lambda^2)^2 e^{2i\omega T_1}} - \frac{3e^{-\frac{\mu_0 s}{2} T_2} P_T \delta e^{i\omega T_1}}{2e^{2i\lambda T_1} (\omega^2 - \lambda^2)} - \frac{3e^{-\frac{\mu_0 s}{2} T_2} P_T \delta}{2e^{2i\lambda T_1} (\omega^2 - \lambda^2) e^{i\omega T_1}} + \frac{3e^{-\frac{\mu_0 s}{4} T_2} P_T^2 \delta^2 e^{2i\omega T_1}}{4e^{i\lambda T_1} (\omega^2 - \lambda^2)^2} + \frac{3e^{-\frac{\mu_0 s}{4} T_2} P_T^2 \delta^2}{4e^{i\lambda T_1} (\omega^2 - \lambda^2)^2 e^{2i\omega T_1}} + e^{-\frac{3\mu_0 s}{4} T_2} e^{3i\lambda T_1} + 3e^{-\frac{3\mu_0 s}{4} T_2} e^{i\lambda T_1} + \frac{3e^{-\frac{3\mu_0 s}{4} T_2}}{e^{i\lambda T_1}} + \frac{e^{-\frac{3\mu_0 s}{4} T_2}}{e^{3i\lambda T_1}} - \frac{P_T^3 \delta^3 e^{3i\omega T_1}}{8(\omega^2 - \lambda^2)^3} - \frac{3P_T^3 \delta^3 e^{i\omega T_1}}{8(\omega^2 - \lambda^2)^3} - \frac{3P_T^3 \delta^3}{8(\omega^2 - \lambda^2)^3 e^{i\omega T_1}} - \frac{P_T^3 \delta^3}{8(\omega^2 - \lambda^2)^3 e^{3i\omega T_1}} + \frac{6e^{-\frac{\mu_0 s}{4} T_2} e^{i\lambda T_1} P_T^2 \delta^2}{4(\omega^2 - \lambda^2)^2} + \frac{6e^{-\frac{\mu_0 s}{4} T_2} P_T^2 \delta^2}{4e^{i\lambda T_1} (\omega^2 - \lambda^2)^2}$$

References

1. Curiel, E. The many definitions of a black hole. *Nat. Astron.* **2019**, *3*, 27–34. [CrossRef]
2. Pati, S.K.; Nayak, B.; Singh, L.P. Black hole dynamics in power-law based metric $f(R)$ gravity. *Gen. Relativ. Gravit.* **2020**, *52*, 78. [CrossRef]
3. Dehyadegari, A.; Sheykhi, A.; Montakhab, A. Critical behavior and microscopic structure of charged AdS black holes via an alternative phase space. *Phys. Lett.* **2017**, *768*, 235–240. [CrossRef]
4. Yazdikarimi, H.; Sheykhi, A.; Dayyani, Z. Critical behavior of Gauss-Bonnet black holes via an alternative phase space. *Phys. Rev.* **2019**, *99*, 124017. [CrossRef]
5. Zhang, L.C.; Ma, M.S.; Zhao, H.H.; Zhao, R. Thermodynamics of phase transition in higher-dimensional Reissner-Nordström-de Sitter black hole. *Eur. Phys. J.* **2014**, *74*, 3052. [CrossRef]
6. Dehghani, M. Three-dimensional scalar-tensor black holes with conformally invariant electrodynamics. *Phys. Rev.* **2019**, *100*, 084019. [CrossRef]
7. Kumar, A.; Singh, D.V.; Ghosh, S.G. D -dimensional Bardeen-AdS black holes in Einstein-Gauss-Bonnet theory. *Eur. Phys. J.* **2019**, *79*, 275. [CrossRef]
8. Dehghani, M.H.; Hendi, S.H.; Sheykhi, A.; Rastegar Sedeqi, H. Thermodynamics of rotating black branes in Einstein-Born-Infeld-dilaton gravity. *J. Cosmol. Astropart. Phys.* **2007**, *2*, 020. [CrossRef]
9. Ghosh, S.G.; Singh, D.V.; Maharaj, S.D. Regular black holes in Einstein-Gauss-Bonnet gravity. *Phys. Rev. D* **2018**, *97*, 104050. [CrossRef]

10. Wang, P.; Wu, H.W.; Yang, H.T. Thermodynamics and phase transition of a nonlinear electrodynamic black hole in a cavity. *J. High Energy Phys.* **2019**, *2019*, 2. [[CrossRef](#)]
11. Wang, P.; Wu, H.W.; Yang, H.T. Thermodynamics and phase transitions of nonlinear electrodynamic black holes in an extended phase space. *J. Cosmol. Astropart. Phys.* **2019**, *2019*, 052. [[CrossRef](#)]
12. Han, Y.W.; Hu, X.Y.; Lan, M.J. Thermodynamics and weak cosmic censorship conjecture in (2+1)-dimensional regular black hole with nonlinear electrodynamic sources. *Eur. Phys. J. Plus* **2020**, *135*, 172. [[CrossRef](#)]
13. Hendi, S.H.; Azari, F.; Rahimi, E.; Elahi, M.; Owjifard, Z.; Armanfard, Z. Thermodynamics and the phase transition of topological dilatonic Lifshitz-like black holes. *Ann. Phys.* **2020**, *532*, 2000162. [[CrossRef](#)]
14. Hendi, S.H.; Panah, B.E.; Panahiyan, S. Thermodynamical structure of AdS black holes in massive gravity with stringy gauge-gravity corrections. *Class. Quantum Gravity* **2017**, *33*, 235007. [[CrossRef](#)]
15. Sherkatghanad, Z.; Mirza, B.; Mirzaeyan, Z.; Mansoori, S.A.H. Critical behaviors and phase transitions of black holes in higher order gravities and extended phase spaces. *Int. J. Mod. Phys. D* **2017**, *26*, 1750017. [[CrossRef](#)]
16. Zhao, Z.W.; Xiu, Y.H.; Li, N. Throttling process of the Kerr-Newman-anti-de Sitter black holes in the extended phase space. *Phys. Rev. D* **2018**, *98*, 124003. [[CrossRef](#)]
17. Ghaffarnejad, H.; Yaraie, E. Effects of a cloud of strings on the extended phase space of Einstein-Gauss-Bonnet AdS black holes. *Phys. Lett. B* **2018**, *785*, 105–111. [[CrossRef](#)]
18. Chen, D.Y. Thermodynamics and weak cosmic censorship conjecture in extended phase spaces of anti-de Sitter black holes with particles' absorption. *Eur. Phys. J. C* **2019**, *79*, 353. [[CrossRef](#)]
19. Qian, W.L.; Lin, K.; Wu, J.P.; Zhang, M.; Yang, Z.Y.; Zou, D.C.; Xu, W.; Yue, R.H. P - V criticality of AdS black hole in the Einstein-Maxwell-power-Yang-Mills gravity. *Gen. Relativ. Gravit.* **2014**, *47*, 14.
20. Nam, C.H. Extended phase space thermodynamics of regular charged AdS black hole in Gauss-Bonnet gravity. *Gen. Relativ. Gravit.* **2019**, *51*, 100. [[CrossRef](#)]
21. Hu, Y.P.; Zeng, H.A.; Jiang, Z.M.; Zhang, H. P - V criticality in the extended phase space of black holes in Einstein-Horndeski gravity. *Phys. Rev. D* **2019**, *100*, 084004. [[CrossRef](#)]
22. Dehghani, M. Thermal fluctuations of AdS black holes in three-dimensional rainbow gravity. *Phys. Lett. B* **2019**, *793*, 234–239. [[CrossRef](#)]
23. Singh, B.K.; Singh, R.P.; Singh, D.V. Extended phase space thermodynamics of Bardeen black hole in massive gravity. *Eur. Phys. J. Plus* **2020**, *135*, 862. [[CrossRef](#)]
24. Singh, B.K.; Singh, R.P.; Singh, D.V. P - v criticality, phase structure and extended thermodynamics of AdS ABG black holes. *Eur. Phys. J. Plus* **2021**, *136*, 575. [[CrossRef](#)]
25. Singh, D.V.; Siwach, S. Thermodynamics and P - v criticality of Bardeen-AdS Black Hole in 4- D Einstein-Gauss-Bonnet Gravity. *Phys. Lett. B* **2020**, *808*, 135658. [[CrossRef](#)]
26. Emparan, R. Higher-dimensional black hole solutions, approximate methods. *Gen. Relativ. Gravit.* **2014**, *46*, 1686. [[CrossRef](#)]
27. Huang, H.; Fan, Z.Y.; Lü, H. Static and dynamic charged black holes. *Eur. Phys. J. C* **2019**, *79*, 975. [[CrossRef](#)]
28. Dehghani, M. Thermodynamic properties of novel black hole solutions in the Einstein-Born-Infeld-dilaton gravity theory. *Eur. Phys. J. C* **2020**, *80*, 996. [[CrossRef](#)]
29. Toshmatov, B.; Ahmedov, B.; Abdurjabbarov, A.; Stuchlík, Z. Rotating regular black hole solution. *Phys. Rev. D* **2014**, *89*, 104017. [[CrossRef](#)]
30. Hendi, S.H.; Dehghani, A. Criticality and extended phase space thermodynamics of AdS black holes in higher curvature massive gravity. *Eur. Phys. J. C* **2019**, *79*, 227. [[CrossRef](#)]
31. Dehghani, M. Nonlinearly charged AdS black hole solutions in three-dimensional massive gravity's rainbow. *Phys. Lett. B* **2020**, *803*, 135335. [[CrossRef](#)]
32. Hendi, S.H. Asymptotic charged BTZ black hole solutions. *J. High Energy Phys.* **2012**, *2012*, 065. [[CrossRef](#)]
33. Bazeia, D.; Brito, F.A.; Costa, F.G. Two-dimensional Hořava-Lifshitz black hole solutions. *Phys. Rev. D* **2015**, *91*, 044026. [[CrossRef](#)]
34. Abishev, M.E.; Boshkayev, K.A.; Dzhunushaliev, V.D.; Ivashchuk, V.D. Dilatonic dyon black hole solutions. *Class. Quantum Gravity* **2015**, *32*, 165010. [[CrossRef](#)]
35. Xu, W. Exact anyon black hole solutions. *Eur. Phys. J. C* **2018**, *78*, 871. [[CrossRef](#)]
36. Yu, S.; Gao, C. Exact black hole solutions with nonlinear electrodynamic field. *Int. J. Mod. Phys. D* **2020**, *29*, 20500327. [[CrossRef](#)]
37. Ayón-Beato, E.; García, A. Four-parametric regular black hole solution. *Gen. Relativ. Gravit.* **2005**, *37*, 635–641. [[CrossRef](#)]
38. Sheykhi, A.; Allahverdizadeh, M. Higher dimensional charged rotating dilaton black holes. *Gen. Relativ. Gravit.* **2010**, *42*, 367–379. [[CrossRef](#)]
39. Sheykhi, A.; Kazemi, A. Higher dimensional dilaton black holes in the presence of exponential nonlinear electrodynamic. *Phys. Rev. D* **2014**, *90*, 044028. [[CrossRef](#)]
40. Sheykhi, A.; Hajkhalili, S. Dilaton black holes coupled to nonlinear electrodynamic field. *Phys. Rev. D* **2014**, *89*, 104019. [[CrossRef](#)]
41. Sheykhi, A. Charged rotating dilaton black strings in (A)dS spaces. *Phys. Rev. D* **2008**, *78*, 064055. [[CrossRef](#)]
42. Sheykhi, A. Magnetic dilaton strings in anti-de Sitter spaces. *Phys. Lett. B* **2009**, *672*, 101–105. [[CrossRef](#)]
43. Sheykhi, A. Rotating black holes in Einstein-Maxwell-dilaton gravity. *Phys. Rev. D* **2008**, *77*, 104022. [[CrossRef](#)]
44. Lessa, L.A.; Silva, J.E.G.; Maluf, R.V.; Almeida, C.A.S. Modified black hole solution with a background Kalb-Ramond field. *Eur. Phys. J. C* **2020**, *80*, 335. [[CrossRef](#)]

45. Dimakis, N.; Leon, G.; Paliathanasis, A. Exact black hole solutions in Einstein-aether scalar field theory. *Phys. Rev. D* **2021**, *103*, 044001. [[CrossRef](#)]
46. Poshteh, M.B.J.; Riazi, N. Phase transition and thermodynamic stability in extended phase space and charged Hořava-Lifshitz black holes. *Gen. Relativ. Gravit.* **2017**, *49*, 64. [[CrossRef](#)]
47. Hendi, S.H.; Panah, B.E.; Panahiyan, S.; Liu, H.; Meng, X. Black holes in massive gravity as heat engines. *Phys. Lett. B* **2018**, *781*, 40–47. [[CrossRef](#)]
48. Chabab, M.; El Mounni, H.; Iraoui, S.; Masmarr, K. Phase transitions and geothermodynamics of black holes in dRGT massive gravity. *Eur. Phys. J. C* **2019**, *79*, 342. [[CrossRef](#)]
49. Khan, I.A.; Ali, F.; Islam, S.; Khan, A.S. The role of the cosmological constant in dynamics of the particle in the Schwarzschild black hole. *Phys. Scr.* **2020**, *95*, 065003. [[CrossRef](#)]
50. Sharif, M.; Shahzadi, M. Particle dynamics near Kerr-MOG black hole. *Eur. Phys. J. C* **2017**, *77*, 363. [[CrossRef](#)]
51. Rác, I. Can we prescribe the physical parameters of multiple black holes? *Mathematics* **2021**, *9*, 3170. [[CrossRef](#)]
52. Qian, W.L.; Lin, K.; Wu, J.P.; Wang, B.; Yue, R.H. On quasinormal frequencies of black hole perturbations with an external source. *Eur. Phys. J. C* **2020**, *80*, 959. [[CrossRef](#)]
53. Charmousis, C.; Crisostomi, M.; Langlois, D.; Noui, K. Perturbations of a rotating black hole in DHOST theories. *Class. Quantum Gravity* **2019**, *36*, 235008. [[CrossRef](#)]
54. Rham, C.D.; Zhang, J. Perturbations of stealth black holes in degenerate higher-order scalar-tensor theories. *Phys. Rev. D* **2019**, *100*, 124023. [[CrossRef](#)]
55. Shafiq, S.; Hussain, S.; Ozair, M.; Aslam, A.; Hussain, T. Charged particle dynamics in the surrounding of Schwarzschild anti-de Sitter black hole with topological defect immersed in an external magnetic field. *Eur. Phys. J. C* **2020**, *80*, 744. [[CrossRef](#)]
56. Wang, R.F.; Gao, F.B. Analytical solution and quasi-periodic behavior of a charged dilaton black hole. *Universe* **2021**, *7*, 377. [[CrossRef](#)]
57. Zhang, Y.P.; Wei, S.W.; Liu, Y.X. Spinning test particle in four-dimensional Einstein-Gauss-Bonnet black holes. *Universe* **2020**, *6*, 103. [[CrossRef](#)]
58. Deng, X.M. Periodic orbits around brane-world black holes. *Eur. Phys. J. C* **2020**, *80*, 489. [[CrossRef](#)]
59. Jawad, A.; Ali, F.; Shahzad, M.U.; Abbas, G. Dynamics of particles around time conformal Schwarzschild black hole. *Eur. Phys. J. C* **2016**, *76*, 586. [[CrossRef](#)]
60. Sharif, M.; Iftikhar, S. Dynamics of particles near black hole with higher dimensions. *Eur. Phys. J. C* **2016**, *76*, 404. [[CrossRef](#)]
61. Wei, S.W.; Yang, J.; Liu, Y.X. Geodesics and periodic orbits in Kehagias-Sfetsos black holes in deformed Hořava-Lifshitz gravity. *Phys. Rev. D* **2019**, *99*, 104016. [[CrossRef](#)]
62. Gao, F.B.; Llibre, J. Global dynamics of Hořava-Lifshitz cosmology with non-zero curvature and a wide range of potentials. *Eur. Phys. J. C* **2020**, *80*, 137. [[CrossRef](#)]
63. Gao, F.B.; Llibre, J. Global dynamics of the Hořava-Lifshitz cosmological system. *Gen. Relativ. Gravit.* **2019**, *51*, 152. [[CrossRef](#)]
64. Liu, C.Q.; Ding, C.K.; Jing, J.L. Periodic orbits around Kerr Sen black holes. *Commun. Theor. Phys.* **2019**, *12*, 1461–1468. [[CrossRef](#)]
65. Ingram, A.R.; Motta, S.E. A review of quasi-periodic oscillations from black hole X-ray binaries, Observation and theory. *New Astron. Rev.* **2019**, *85*, 101524. [[CrossRef](#)]
66. Kolo, M.; Shahzadi, M.; Stuchlík, Z. Quasi-periodic oscillations around Kerr-MOG black holes. *Eur. Phys. J. C* **2020**, *80*, 133. [[CrossRef](#)]
67. Nayfeh, A.H.; Mook, D.T. *Nonlinear Oscillations*; Wiley-VCH: Hoboken, NJ, USA, 1995.
68. Dai, C.Q.; Chen, S.B.; Jing, J.L. Thermal chaos of a charged dilaton-AdS black hole in the extended phase space. *Eur. Phys. J. C* **2020**, *80*, 245. [[CrossRef](#)]
69. Sheykhi, A. Thermodynamics of charged topological dilaton black holes. *Phys. Rev. D* **2007**, *76*, 124025. [[CrossRef](#)]
70. Sheykhi, A. Topological Born-Infeld-dilaton black holes. *Phys. Lett. B* **2008**, *662*, 7–13. [[CrossRef](#)]
71. Dehyadegari, A.; Sheykhi, A.; Montakhab, A. Novel phase transition in charged dilaton black holes. *Phys. Rev. D* **2017**, *96*, 084012. [[CrossRef](#)]
72. Dehghani, M.H.; Kamrani, S.; Sheykhi, A. P - V criticality of charged dilatonic black holes. *Phys. Rev. D* **2014**, *90*, 104020. [[CrossRef](#)]
73. Dehyadegari, A.; Sheykhi, A. Critical behavior of charged dilaton black holes in AdS space. *Phys. Rev. D* **2020**, *102*, 064021. [[CrossRef](#)]
74. Li, A.C.; Shi, H.Q.; Zeng, D.F. Phase structure and quasinormal modes of a charged AdS dilaton black hole. *Phys. Rev. D* **2018**, *97*, 026014. [[CrossRef](#)]
75. Chen, Y.; Li, H.T.; Zhang, S.J. Chaos in Born-Infeld-AdS black hole within extended phase space. *Gen. Relativ. Gravit.* **2019**, *51*, 134. [[CrossRef](#)]
76. Chabab, M.; Mounni, H.E.; Iraoui, S.; Masmarr, K.; Zhizeh, S. Chaos in charged AdS black hole extended phase space. *Phys. Lett. B* **2018**, *78*, 316–321. [[CrossRef](#)]
77. Mahish, S.; Bhamidipati, C. Chaos in charged Gauss-Bonnet AdS black holes in extended phase space. *Phys. Rev. D* **2019**, *99*, 106012. [[CrossRef](#)]